Mechanism and Machine Theory 75 (2014) 161–176

Contents lists available at ScienceDirect

Mechanism and Machine Theory

journal homepage: www.elsevier.com/locate/mechmt

The 3-RPS parallel manipulator from an algebraic viewpoint

J. Schadlbauer, D.R. Walter, M.L. Husty *

University of Innsbruck, Austria

ARTICLE INFO

Article history:
Received 3 February 2013
Received in revised form 19 October 2013
Accepted 2 December 2013
Available online 23 January 2014

Keywords:
3-RPS parallel manipulator
Algebraic geometry
Kinematic mapping
Study-parameters
Operation modes
Singular poses

ABSTRACT

The 3-RPS parallel manipulator is a three degree of freedom parallel manipulator, which was introduced by K. Hunt in 1983 as one of the lower mobility parallel manipulators. Since then the 3-RPS gained a lot of attention in literature, but most of the articles on this manipulator use screw theory to explain its local kinematic behavior. An algebraic approach via *Study's kinematic mapping* reveals interesting global properties of this type of manipulator. The global kinematic behavior of the manipulator is described by algebraic equations, so called *constraint equations*. In the kinematic analysis these equations are manipulated using methods of algebraic geometry and are interpreted geometrically. It is shown, that the forward kinematics of the 3-RPS has in general 16 solutions in the field of complex numbers. Its workspace splits into two, essentially different *operation modes*. A geometric and kinematic interpretation of both modes is given. Furthermore it is shown that a transition between the operation modes is possible under certain circumstances. The operation modes are detected via a *primary decomposition* of the ideal corresponding to the constraint equations. Conditions for *singular poses* are derived from the constraint equations by discussing the Jacobian of the set of constraint equations. Finally, for singular poses of each operation mode as well as for singular poses belonging to both operation modes, a mapping into the space of joint parameters will be described. Images of singular poses of the manipulator under the mapping determine algebraic surfaces in the joint space, which are analyzed algebraically.

1. Introduction

A 3-RPS parallel manipulator is a three degree of freedom (3-DOF) parallel manipulator. This type of manipulator was introduced by K. Hunt in 1983 as one of the lower mobility parallel manipulators [1]. The 3-RPS parallel manipulator consists of a basis and a moving platform, which are connected with three identical RPS legs, where the rotational joints (R-joints) are attached to the base and the spherical joints (S-joints) are attached to the moving platform. The leg lengths are adjustable by prismatic joints (P-joints), generating a coupled 3-DOF motion of the moving platform (see Fig. 1). In the past few years many papers were published dealing with the 3-RPS manipulator. Tsai [2] and Nanua et al. [3] found the correct number of solutions of the direct kinematics, a fact which is also mentioned by Gallardo et al. in Ref. [4] and Bonev in Ref. [5]. Bonev also mentioned two different modes of operation in Ref. [5]. Gallardo et al. [4] and Fang and Huang [6] discuss the velocity as well as the acceleration behavior using loop closure equations and numerical methods. Moreover, inverse kinematics and dynamics were studied by Ibrahim and Khalil [7], Sokolov and Xirouchakis [8], Dasgupta and Choudhury [9] and Song et al. [10]. A paper about the identification of dynamic parameters was published by Farhat et al. [11], validating their results by practical examples. The

* Corresponding author. Tel.: +43 51250761200; fax: +43 51250761299.
E-mail addresses: josef.schadlbauer@uibk.ac.at (J. Schadlbauer), csab6729@gmx.at (D.R. Walter), manfred.husty@uibk.ac.at (M.L. Husty).

0094-114X/$ – see front matter © 2013 Elsevier Ltd. All rights reserved.
http://dx.doi.org/10.1016/j.mechmachtheory.2013.12.007

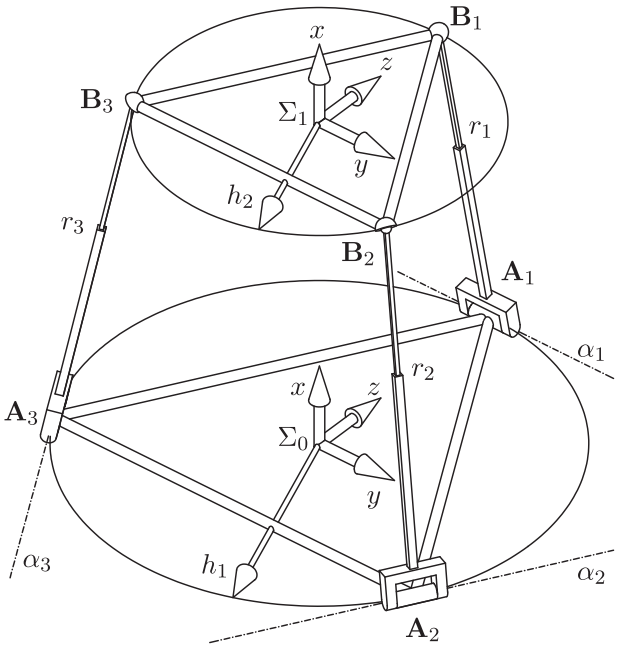

Fig. 1. Basic architecture of the 3-RPS parallel manipulator.

contributions of Huang et.al. brought lot of interesting insights in the local kinematic behavior of the 3-RPS manipulator: In Ref. [12] they discuss some special configurations of the manipulator, e.g. when the platform stays parallel to the base, in Ref. [13] they provide a method for the identification of the principle screws in the third order screw system generated by this manipulator and in Ref. [14] they discuss the possible motion characteristics when the linear displacements of the platform of the 3-RPS manipulator are restricted. The dimensional synthesis problem was treated by Mohan Rao and Mallikajuba Rao in Ref. [15]. Lu and Leinonen [16] even connected two 3-RPS parallel manipulators in series to generate a more complicated motion. Singular poses of the manipulator were treated by Basu and Ghosal [17], Zlatanov et al. [18], Sokolov and Xirouchakis [19], and Liu and Cheng [20], but because of the local character of screw theory some singular poses are missing. A classification of self-motions via the algebraic representation of the 3-RPS is treated in the recent paper by Husty et al. [21].

In this contribution a special design of the 3-RPS parallel manipulator will be considered. The basis and the moving platform are equilateral triangles and the rotational axes at the base are tangent to the circumcircle of the base triangle. The main objective of this work is to give a complete algebraic description of this manipulator using *Study's kinematic mapping* in combination with methods of algebraic geometry. In this case the manipulator's constraints will be expressed by algebraic equations. Inherent in this algebraic description is the complete motion of this manipulator. Another property of this algebraic representation is that the direct kinematics can be solved globally. Two operation modes are found and all singular poses of both operation modes are discussed in detail. Finally, the transition between these operation modes will be described.

The structure of this paper is as follows: In Section 2 a complete description of the manipulator will be given. Deriving the constraint equations, which is one of the fundamental steps, is content of Section 3. Solving the equations and determining the number of solutions is the topic of Section 4, at which Section 4.1 is treating the case of arbitrary limb lengths and Section 4.2 solves the case of equal limb lengths. The different operation modes are discussed in detail and interpreted geometrically in Section 5. Section 6 is devoted to a complete treatment of singular poses of this manipulator. The transition between the operation modes is the topic of Section 6.1. In the final Section 7 the singularity set is analyzed algebraically.

2. Design of the manipulator

Fig. 1 displays the architecture of the studied manipulator: The base of the manipulator consists of an equilateral triangle with vertices $\mathbf{A}_1$, $\mathbf{A}_2$ and $\mathbf{A}_3$. The circumradius of the triangle $\mathbf{A}_1\mathbf{A}_2\mathbf{A}_3$ is h_1 and the center coincides with the origin of Σ_0, the fixed frame. Furthermore, the plane determined by $\mathbf{A}_1$, $\mathbf{A}_2$ and $\mathbf{A}_3$ is defined as the yz-plane of the fixed frame. Finally, the point $\mathbf{A}_1$ lies on the z-axis and the point $\mathbf{A}_2$ lies on the positive side of the y-axis of Σ_0. The situation in the moving frame is completely analog. The equilateral triangle $\mathbf{B}_1\mathbf{B}_2\mathbf{B}_3$ has a circumcircle with radius h_2, and again the center coincides with the origin of Σ_1, the moving

frame. The yz-plane of Σ_1 coincides with the plane defined by $\mathbf{B}_1$, $\mathbf{B}_2$ and $\mathbf{B}_3$. Finally the point $\mathbf{B}_1$ lies on the z-axis and $\mathbf{B}_2$ lies on the positive side of the y-axis of Σ_1.

Now each pair of vertices $\mathbf{A}_i\mathbf{B}_i$ ($i\in\{1,2,3\}$) is connected by a limb with an R-joint in $\mathbf{A}_i$ and an S-joint in $\mathbf{B}_i$. The axes α_i of the R-joints in $\mathbf{A}_i$ are tangent to the circumcircle of the triangle $\mathbf{A}_1\mathbf{A}_2\mathbf{A}_3$ and therefore lie in the yz-plane of Σ_0. The R-joints are connected via actuated P-joints with the S-joints. The lengths of the P-joints are denoted by r_i.

Overall there are five parameters, namely h_1, h_2, r_1, r_2 and r_3. While h_1 and h_2 determine the design of the manipulator, the parameters r_1, r_2 and r_3 are joint parameters, which define the motion of the manipulator. The joint parameters can be assumed to be like design parameters when they are assigned with specific leg lengths r_i. The design parameters h_1 and h_2 are chosen to be strictly positive real numbers, while the joint parameters r_1, r_2 and r_3 are also allowed to become zero. From this point of view a complete discussion of the direct kinematics of this manipulator will be given.

3. Deduction of constraint equations

A first essential step in the kinematic analysis of a manipulator is the computation of constraint equations. To compute these equations which describe all the possible solutions of the direct kinematics, i.e. all poses of Σ_1 with respect to Σ_0 and with that all poses of the platform (or the workspace), the *Study-parametrization* of the special Euclidean group SE(3) is used. The vertices of the base triangle and the platform triangle in Σ_0 respectively (resp.) Σ_1 are

$$\mathbf{A}_1=(1:0:0:h_1),\quad \mathbf{A}_2=\left(1:0:\sqrt{3}h_1/2:-h_1/2\right),\quad \mathbf{A}_3=\left(1:0:-\sqrt{3}h_1/2:-h_1/2\right),$$
$$\mathbf{b}_1=(1:0:0:h_2),\quad \mathbf{b}_2=\left(1:0:\sqrt{3}h_2/2:-h_2/2\right),\quad \mathbf{b}_3=\left(1:0:-\sqrt{3}h_2/2:-h_2/2\right),$$

thereby using a projective coordinate system with the homogenizing coordinate written on first place. To avoid confusion coordinates with respect to the fixed frame Σ_0 are written in capital bold letters, while coordinates with respect to the moving frame Σ_1 are denoted by lower case letters.

To obtain the coordinates $\mathbf{B}_1$, $\mathbf{B}_2$ and $\mathbf{B}_3$ of $\mathbf{b}_1$, $\mathbf{b}_2$ and $\mathbf{b}_3$ with respect to Σ_0 a coordinate transformation has to be applied. To describe this coordinate transformation in an algebraic way the Study-parametrization of the special Euclidean group SE(3) is used (for detailed information to this approach see [22]). In this parametrization every matrix $\mathbf{M}\in$SE(3) can be represented by

$$\mathbf{M}=\begin{pmatrix} x_0^2+x_1^2+x_2^2+x_3^2 & 0^T\\ \mathbf{M}_T & \mathbf{M}_R\end{pmatrix},\quad \mathbf{M}_T=\begin{pmatrix} 2(-x_0y_1+x_1y_0-x_2y_3+x_3y_2)\\ 2(-x_0y_2+x_1y_3+x_2y_0-x_3y_1)\\ 2(-x_0y_3-x_1y_2+x_2y_1+x_3y_0)\end{pmatrix},$$
$$\mathbf{M}_R=\begin{pmatrix} x_0^2+x_1^2-x_2^2-x_3^2 & 2(x_1x_2-x_0x_3) & 2(x_1x_3+x_0x_2)\\ 2(x_1x_2+x_0x_3) & x_0^2-x_1^2+x_2^2-x_3^2 & 2(x_2x_3-x_0x_1)\\ 2(x_1x_3-x_0x_2) & 2(x_2x_3+x_0x_1) & x_0^2-x_1^2-x_2^2+x_3^2\end{pmatrix},$$

where $\mathbf{M}_T$ represents the translational part and $\mathbf{M}_R$ represents the rotational part of $\mathbf{M}$. The parameters x_i, y_i ($i\in\{0,\ldots,3\}$) which appear in this parametrization of $\mathbf{M}$ are the so called *Study-parameters* of the transformation $\mathbf{M}$. The mapping

$$\kappa: SE(3)\to P\in\mathbb{P}^7$$
$$\mathbf{M}(x_i,y_i)\mapsto(x_0:x_1:x_2:x_3:y_0:y_1:y_2:y_3)\neq(0:0:0:0:0:0:0:0)$$

is called *Study's kinematic mapping* and it maps every displacement in SE(3) to a point P in a 7-dimensional projective space $\mathbb{P}^7$, the *kinematic image space*. A point $P=(x_0:x_1:x_2:x_3:y_0:y_1:y_2:y_3)\in\mathbb{P}^7$ represents a Euclidean transformation, if and only if it fulfills the following equation and the following inequality

$$x_0y_0+x_1y_1+x_2y_2+x_3y_3=0, \tag{1}$$

$$x_0^2+x_1^2+x_2^2+x_3^2\neq 0. \tag{2}$$

All points which fulfill Eq. (1) lie on a 6-dimensional quadric, the so called *Study quadric* $S_6^2\subset\mathbb{P}^7$. Points which do not fulfill the normalization term in Eq. (2) belong to the 3-dimensional *exceptional generator* $x_0=x_1=x_1=x_1=0$, which is a subset of S_6^2. Points in this exceptional generator do not represent Euclidean displacements of $SE(3)$. The coordinates $\mathbf{B}_i$ of $\mathbf{b}_i$ with respect to Σ_0 are given by

$$\mathbf{B}_i=\mathbf{M}\cdot\mathbf{b}_i,\quad i\in\{1,2,3\}.$$

Now, as the coordinates of all vertices are given in terms of Study-parameters and design parameters, the constraint equations are obtained by examining the design of the manipulator a little bit closer. First of all the limb connecting $\mathbf{A}_i$ and $\mathbf{B}_i$ has to be perpendicular to the axis α_i of the R-joint in $\mathbf{A}_i$, this means that the scalar product of the vector $\mathbf{A}_i\mathbf{B}_i$ and the direction vector of α_i has to vanish. After this computation the common denominator $x_0^2 + x_1^2 + x_2^2 + x_3^2$ can be removed and the following three equations are obtained

$$\begin{aligned}
\widetilde{g}_1: &\quad x_0y_2 - x_1y_3 - x_2y_0 + x_3y_1 - h_2x_2x_3 + h_2x_0x_1 = 0\\
\widetilde{g}_2: &\quad 4\sqrt{3}h_2x_0x_1 + 2\sqrt{3}h_2x_2x_3 - 2\sqrt{3}x_0y_2 + 2\sqrt{3}x_1y_3 + 2\sqrt{3}x_2y_0 - 2\sqrt{3}x_3y_1\\
&\qquad + 3h_2x_2^2 - 3h_2x_3^2 - 6x_0y_3 - 6x_1y_2 + 6x_2y_1 + 6x_3y_0 = 0\\
\widetilde{g}_3: &\quad 4\sqrt{3}h_2x_0x_1 + 2\sqrt{3}h_2x_2x_3 - 2\sqrt{3}x_0y_2 + 2\sqrt{3}x_1y_3 + 2\sqrt{3}x_2y_0 - 2\sqrt{3}x_3y_1\\
&\qquad - 3h_2x_2^2 + 3h_2x_3^2 + 6x_0y_3 + 6x_1y_2 - 6x_2y_1 - 6x_3y_0 = 0,
\end{aligned} \tag{3}$$

which after some elementary manipulations ($g_1 = \frac{1}{3h_2}\left[\frac{1}{4\sqrt{3}}(\widetilde{g}_2 + \widetilde{g}_3) + \widetilde{g}_1\right]$, $g_2 = \frac{1}{6}(\widetilde{g}_2 - \widetilde{g}_3)$, $g_3 = \frac{1}{4\sqrt{3}}(\widetilde{g}_2 + \widetilde{g}_3)$) simplify to

$$\begin{aligned}
g_1: &\quad x_0x_1 = 0\\
g_2: &\quad h_2x_2^2 - h_2x_3^2 - 2x_0y_3 - 2x_1y_2 + 2x_2y_1 + 2x_3y_0 = 0\\
g_3: &\quad 2h_2x_0x_1 + h_2x_2x_3 - x_0y_2 + x_1y_3 + x_2y_0 - x_3y_1 = 0.
\end{aligned} \tag{4}$$

In the direct kinematics constant values are assigned to all joint parameters, therefore the Euclidean distance between $\mathbf{A}_i$ and $\mathbf{B}_i$ has to be $r_i = const$, e.g. $\|\mathbf{A}_i\mathbf{B}_i\|^2 = r_i^2$. The corresponding constraint equations have been derived in Refs. [23,24] for the solution of the direct kinematics of the 6-SPS-Stewart–Gough-platform. Substituting the design parameters of the 3-RPS into this formula the following distance equations are obtained

$$\begin{aligned}
g_4: &\ (h_1-h_2)^2x_0^2 + (h_1+h_2)^2x_1^2 + (h_1+h_2)^2x_2^2 + (h_1-h_2)^2x_3^2\\
&\ +4(h_1-h_2)x_0y_3 + 4(h_1+h_2)x_1y_2 - 4(h_1+h_2)x_2y_1\\
&\ -4(h_1-h_2)x_3y_0 + 4\left(y_0^2+y_1^2+y_2^2+y_3^2\right) - \left(x_0^2+x_1^2+x_2^2+x_3^2\right)r_1^2 = 0\\
g_5: &\ (h_1-h_2)^2x_0^2 + (h_1+h_2)^2x_1^2 + \left(h_1^2+h_2^2-h_1h_2\right)x_2^2 + \left(h_1^2+h_2^2+h_1h_2\right)x_3^2 - 2(h_1-h_2)x_0y_3 - 2(h_1+h_2)x_1y_2\\
&\ +2(h_1+h_2)x_2y_1 + 2(h_1-h_2)x_3y_0 - 2\sqrt{3}(h_1-h_2)x_0y_2 + 2\sqrt{3}(h_1+h_2)x_1y_3 + 2\sqrt{3}(h_1-h_2)x_2y_0\\
&\ -2\sqrt{3}(h_1+h_2)x_3y_1 - 2\sqrt{3}h_1h_2x_2x_3 + 4\left(y_0^2+y_1^2+y_2^2+y_3^2\right) - \left(x_0^2+x_1^2+x_2^2+x_3^2\right)r_2^2 = 0\\
g_6: &\ (h_1-h_2)^2x_0^2 + (h_1+h_2)^2x_1^2 + \left(h_1^2+h_2^2-h_1h_2\right)x_2^2 + \left(h_1^2+h_2^2+h_1h_2\right)x_3^2 - 2(h_1-h_2)x_0y_3 - 2(h_1+h_2)x_1y_2\\
&\ +2(h_1+h_2)x_2y_1 + 2(h_1-h_2)x_3y_0 + 2\sqrt{3}(h_1-h_2)x_0y_2 - 2\sqrt{3}(h_1+h_2)x_1y_3 - 2\sqrt{3}(h_1-h_2)x_2y_0\\
&\ +2\sqrt{3}(h_1+h_2)x_3y_1 + 2\sqrt{3}h_1h_2x_2x_3 + 4\left(y_0^2+y_1^2+y_2^2+y_3^2\right) - \left(x_0^2+x_1^2+x_2^2+x_3^2\right)r_3^2 = 0.
\end{aligned}$$

Geometrically the six equations mean that the points $\mathbf{B}_i$ have the freedom to move on circles with center $\mathbf{A}_i$ and radii r_i in planes perpendicular to the axes α_i. Keeping in mind that every solution has to represent a transformation in $SE(3)$, the equation of the Study quadric Eq. (1) has to be added to the system ($g_7 : x_0y_0 + x_1y_1 + x_2y_2 + x_3y_3 = 0$). Solving the direct kinematics means to find all points in $\mathbb{P}^7$ which fulfill the set of equations $\{g_1, \ldots, g_7\}$, taking into account that $x_0^2 + x_1^2 + x_2^2 + x_3^2 \neq 0$. As the coordinates in $\mathbb{P}^7$ are homogeneous, there is still the freedom to normalize. In order to exclude the exceptional generator from the solutions this normalization is chosen to be $g_8 : x_0^2 + x_1^2 + x_2^2 + x_3^2 - 1 = 0$. Now it has to be taken into account that every projective solution has two affine representatives. This has to be kept in mind when counting the solutions of the direct kinematics. The constraint equations could have been computed too using the linear implicitization algorithm developed by Walter and Husty in Ref. [25].

4. Solving the direct kinematics

The solutions of the eight constraint equations $\{g_1,g_2,g_3,g_4,g_5,g_6,g_7,g_8\}$ derived in the previous section represent all the possible assembly modes or poses of the 3-RPS parallel manipulator depending on the design parameters h_1, h_2 and on the active joint parameters r_1, r_2 and r_3. To handle this system of equations neatly, methods of algebraic geometry are applied (see e.g. [26] for basics in algebraic geometry). In the following the list of equations is always written as a polynomial ideal with variables x_0, x_1, x_2, x_3, y_0, y_1, y_2, y_3 over the coefficient ring $\mathbb{C}[h_1,h_2,r_1,r_2,r_3]$, because in some cases the solutions can become complex, but algebraically still counting as solutions. Furthermore, and without loss of generality, the system is simplified by scaling $h_1 = 1$. To apply methods of algebraic geometry the ideal is now defined as

$$\mathcal{I} = \langle g_1, g_2, g_3, g_4, g_5, g_6, g_7, g_8 \rangle,$$

where g_i denotes the polynomial on the left-hand side of the corresponding equation. The *vanishing set* $\mathbf{V}(\mathcal{I})$ of this ideal $\mathcal{I}$ consists of all points in $\mathbb{P}^7$ for which all the equations vanish, i.e. all the solutions of direct kinematics. The vanishing set of an

ideal is called a *variety*. At this point the following sub-ideal is studied, which is independent of the joint parameters r_1, r_2 and r_3

$$\mathcal{J} = \langle g_1, g_2, g_3, g_7 \rangle.$$

The ideal $\mathcal{J}$ is a rather small ideal. To check if the ideal $\mathcal{J}$ is the intersection of some, maybe smaller ideals a *primary decomposition* is computed. A primary decomposition is computed with the algorithm *primdecGTZ* of the free algebraic manipulation software *Singular* [27]. The primary decomposition then returns some $\mathcal{J}_i$ for which $\mathcal{J} = \cap_i \mathcal{J}_i$. On the other hand the vanishing set is given by $\mathbf{V}(\mathcal{J}) = \cup_i \mathbf{V}(\mathcal{J}_i)$. Geometrically the primary decomposition tells if the variety is the union of some other "maybe simpler" varieties. At this point the correspondence between an ideal and the variety of an ideal should be clear.

For the 3-RPS manipulator the vanishing sets $\mathbf{V}(\langle g_i \rangle)$ ($i \in \{1,2,3,7\}$) of the equations g_1, g_2, g_3 and g_7 describe quadrics in $\mathbb{P}^7$. Therefore a primary decomposition would tell that the intersection of these quadrics splits into smaller pieces. And indeed, the result of the primary decomposition shows that the ideal $\mathcal{J}$ decomposes into three components $\mathcal{J}_i$

$$\mathcal{J} = \bigcap_{i=1}^{3} \mathcal{J}_i,$$

with

$$\begin{aligned}
\mathcal{J}_1 &= \left\langle x_0, x_1y_1 + x_2y_2 + x_3y_3, h_2x_2^2 - h_2x_3^2 - 2x_1y_2 + 2x_2y_1 + 2x_3y_0, h_2x_2x_3 + x_1y_3 + x_2y_0 - x_3y_1 \right\rangle \\
\mathcal{J}_2 &= \left\langle x_1, x_0y_0 + x_2y_2 + x_3y_3, h_2x_2^2 - h_2x_3^2 - 2x_0y_3 + 2x_2y_1 + 2x_3y_0, h_2x_2x_3 - x_0y_2 + x_2y_0 - x_3y_1 \right\rangle \\
\mathcal{J}_3 &= \langle x_0, x_1, x_2, x_3 \rangle.
\end{aligned} \tag{5}$$

Inspection of the vanishing set $\mathbf{V}(\mathcal{J}_3 \cup \langle g_8 \rangle)$ yields the result that it is empty, because the set of polynomials $\{x_0, x_1, x_2, x_3, x_0^2 + x_1^2 + x_2^2 + x_3^3 - 1\}$ can never vanish simultaneously over $\mathbb{R}$ or $\mathbb{C}$. So only two components are left. To complete the analysis the remaining equations have to be added by writing

$$\mathcal{K}_i = \mathcal{J}_i \cup \langle g_4, g_5, g_6, g_8 \rangle.$$

The vanishing set of $\mathcal{I}$ is now the union

$$\mathbf{V}(\mathcal{I}) = \bigcup_{i=1}^{2} \mathbf{V}(\mathcal{K}_i).$$

Again, it has to be mentioned that adding equations means geometrically to intersect some varieties in $\mathbb{P}^7$. The advantage of this primary decomposition is that every ideal $\mathcal{K}_i$ can be studied separately, which will be the subject of Section 5.

4.1. Number of solutions for arbitrary design parameters

Now the solutions to the direct kinematics for arbitrary design parameters will be given. In this section the five parameters h_i, r_j ($i \in \{1,2\}$, $j \in \{1,2,3\}$) are arbitrary and not assigned with values. Under this assumption it is possible to solve the direct kinematics completely general. The *Hilbert-dimension* is computed separately for $\mathcal{K}_1$ and $\mathcal{K}_2$. It turns out that

$$dim(\mathcal{K}_i) = 0, \qquad i \in \{1,2\},$$

so there are in general (for generic parameter values) only finitely many solutions, or finitely many *assembly modes* of this manipulator. The dimension of an ideal can be computed with the command *dim* in *Singular* [27]. The geometric meaning is that the intersection of the varieties only consists of finitely many points in $\mathbb{P}^7$. Here $dim(\mathcal{K}_i)$ represents the ideal dimension over $\mathbb{C}[h_1, h_2, r_1, r_2, r_3]$ (in difference to the following Section 5). To obtain the solutions an ordered *Gröbner* basis was computed using the *grobner* command in *Singular* [27]. For each component $\mathcal{K}_1$ and $\mathcal{K}_2$ a univariate polynomial of degree eight could be computed without assigning numbers to the design and leg parameters. Because of the fundamental theorem of algebra one could conclude that there exist eight solutions in each component. But substitution shows that there is a quadratic equation left in the back substitution, which is doubling the number of solutions to 16. Taking into account the normalizing condition this number has to be halved again (see Section 3). Therefore the number of solutions is

$$|\mathbf{V}(\mathcal{K}_i)| = 8, \quad i \in \{1,2\}.$$

So in general there exist 16 solutions of the direct kinematics of a 3-RPS parallel manipulator in agreement with [2,4,5,3], when the design parameters h_1 and h_2 and the leg parameters r_1, r_2 and r_3 are chosen arbitrarily.

4.2. Number of solutions for equal leg lengths

In this section the special case of equal leg lengths is discussed:

$$r_1 = r_2 = r_3 = r.$$

Also in this case the Hilbert-dimension can be calculated and yields

$$dim(\mathcal{K}_i) = 0, \qquad i \in \{1,2.\}$$

From this follows that there is also a finite set of solutions. The number of solutions turns out to be

$$|\mathbf{V}(\mathcal{K}_i)| = 4, \qquad i \in \{1,2\}.$$

Therefore there are eight solutions of the direct kinematics in the case of equal leg lengths. The home pose, which is depicted in Fig. 1, belongs to this case and the solution reads:

$$(x_0 : x_1 : x_2 : x_3 : y_0 : y_1 : y_2 : y_3) = \left(1 : 0 : 0 : 0 : 0 : -\sqrt{r^2-(h_1-h_2)^2} : 0 : 0\right).$$

5. Geometric and kinematic interpretation of the operation modes

As shown in Section 4 the workspace of the 3-RPS parallel manipulator decomposes into two components, namely $\mathcal{K}_1$, which is characterized by $x_0 = 0$, resp. $\mathcal{K}_2$, in which $x_1 = 0$. All solutions in $\mathbf{V}(\mathcal{K}_i)$ constitute an *operation mode* of the manipulator. At this point it has to be mentioned that the two operation modes are connected, i.e. there are special solutions which belong to $\mathbf{V}(\mathcal{K}_1)$ and $\mathbf{V}(\mathcal{K}_2)$, having $x_0 = x_1 = 0$. In this section a deeper discussion of the operation modes will be given.

Up to now the joint parameters were treated as fixed parameters because the direct kinematics was discussed, but in this section they are allowed to change, i.e. the P-joints will actuate the manipulator. In this case the Hilbert-dimension treating r_1, r_2 and r_3 as variables is

$$\overline{dim}(\mathcal{K}_i) = 3, \qquad i \in \{1,2\}$$

which means that the manipulator really generates a 3-DOF motion. In difference to $dim(\mathcal{K}_i)$ of Section 4, which denoted the Hilbert-dimension over $\mathbb{C}[h_1,h_2,r_1,r_2,r_3]$, $\overline{dim}(\mathcal{K}_i)$ denotes the Hilbert-dimension over $\mathbb{C}[h_1,h_2]$, because r_1, r_2 and r_3 are now considered variable, additionally to the pose parameters x_0, x_1, x_2, x_3, y_0, y_1, y_2 and y_3.

In the following both operation modes will be studied separately. The conditions $x_0 = 0$, resp. $x_1 = 0$, have a special meaning for the possible motion of the manipulator. Via the inverse kinematic mapping κ^{-1} the 4×4-matrix $\mathbf{M}(x_i,y_i)$ of $SE(3)$ can be reconstructed for every solution in $\mathbf{V}(\mathcal{K}_i)$ $(i \in \{1,2\})$. Every matrix $\mathbf{M} \in SE(3)$ represents a discrete screw motion from the identity, where Σ_0 and Σ_1 are coincident, to the transformed pose of Σ_1 with respect to Σ_0. This result is called the theorem of Chasles. In special situations this motion might also be a pure rotation or translation. A discrete screw motion is the concatenation of a rotation about an axis and a translation along the same axis. From the matrix representation of this discrete screw motion the discrete screw axis (DSA) a, the translational distance s, as well as the angle φ of the rotational part can be computed. But this information can also be obtained directly from the Study-parameters, because they contain the complete information of the transformation itself. If a set of Study-parameters $x_0, \ldots, y_3$, which fulfill Eq. (1), is given, then the *Plücker-coordinates* $L = (p_0 : p_1 : p_2 : p_3 : p_4 : p_5)$ of the corresponding DSA are given by (Weiss [28])

$$\begin{aligned} p_0 &= \left(-x_1^2-x_2^2-x_3^2\right)x_1, \quad p_3 = x_0y_0x_1-\left(-x_1^2-x_2^2-x_3^2\right)y_1, \\ p_1 &= \left(-x_1^2-x_2^2-x_3^2\right)x_2, \quad p_4 = x_0y_0x_2-\left(-x_1^2-x_2^2-x_3^2\right)y_2, \\ p_2 &= \left(-x_1^2-x_2^2-x_3^2\right)x_3, \quad p_5 = x_0y_0x_3-\left(-x_1^2-x_2^2-x_3^2\right)y_3. \end{aligned} \tag{6}$$

The Plücker-coordinates corresponding to lines lie on a quadric $M_4^2 \subset \mathbb{P}^5$, the so called *Plücker* or *Klein quadric*, which is given by

$$p_0p_3 + p_1p_4 + p_2p_5 = 0. \tag{7}$$

For a detailed modern introduction to line geometry see Ref. [29]. The coordinates given in Eq. (6) are really Plücker-coordinates, because the Study-parameters lie in S_6^2 and this yields

$$p_0p_3 + p_1p_4 + p_2p_5 = -\left(x_1^2+x_2^2+x_3^2\right)^2 \underbrace{(x_0y_0 + x_1y_1 + x_2y_2 + x_3y_3)}_{=0} = 0. \tag{8}$$

Furthermore, the angle φ of the rotational part and the distance s of the translational part of the given transformation can be computed from the Study-parameters directly with

$$\cot\left(\frac{\varphi}{2}\right) = \frac{x_0}{\sqrt{x_1^2+x_2^2+x_3^2}} \tag{9}$$

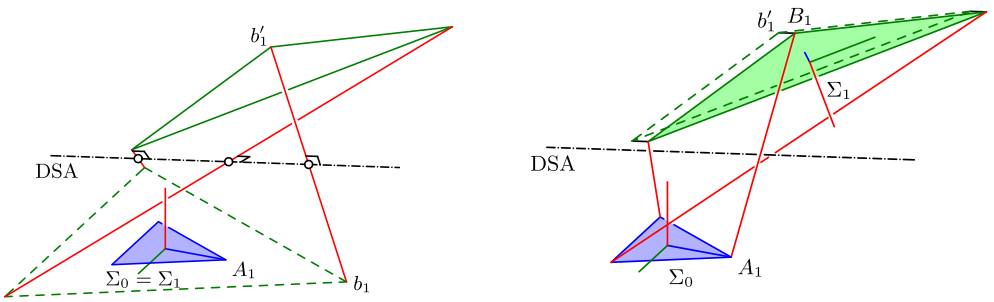

Fig. 2. Discrete screw motion in the operation mode $\mathbf{V}(\mathcal{K}_1)$.

$$s = \frac{y_0}{\sqrt{x_1^2 + x_2^2 + x_3^2}}. \tag{10}$$

Furthermore, if the Study-parameters are normalized ($x_0^2 + x_1^2 + x_2^2 + x_3^2 = 1$) Eq. (9) for the angle φ simplifies to $x_0 = cos(\frac{\varphi}{2})$. The direction vector of the DSA is given by $(p_1,p_2,p_3)^T$ of Eq. (6).

5.1. The operation mode $\mathbf{V}(\mathcal{K}_1)$

In the operation mode $\mathbf{V}(\mathcal{K}_1)$ the condition $x_0 = 0$ has to hold for all poses. The angle φ of the rotational part of the transformation is given by Eq. (9), which means in this case that $\varphi = \pi$. Geometrically all the transformations in this operation mode are discrete screw motions with an angle π. Study called these displacements π-screws [30]. This operation mode does not include pure translations, because $x_0 = 0$ and the condition for pure translation $x_1 = x_2 = x_3 = 0$ yields $x_0 = x_1 = x_2 = x_3 = 0$. The solution would be in the exceptional generator and this yields no valid Euclidean transformation.

In the following example one pose of the manipulator in this operation mode is shown. The design parameters are assigned to be $h_1 = 1$, $h_2 = 3$ (i.e. the basis is smaller than the platform). The joint parameters are chosen to be $r_1 = 3.840$, $r_2 = 7$, $r_3 = 1.712$. One solution of the direct kinematics within this operation mode computed with three digit accuracy is $(x_0 : \ldots : y_3) = (0 : .333 : .500 : .799 : .218 : 1.250 : .648 : -.927)$. This discrete screw motion is the concatenation of a rotation about a DSA with Plücker-coordinates $(p_0 : \ldots : p_5) = (-.333 : -.500 : -.799 : 1.250 : .648 : -.927)$ with an angle $\varphi = \pi$ and a translation along the screw axis with translational distance $s = .437$. In the left picture of Fig. 2 the π-turn (a pure rotation with an angle π) about the DSA from the identity (dashed triangle) to the rotated triangle is shown. Note that the lines connecting corresponding points of the dashed and the rotated triangle (e.g. b_1 and b_1') intersect the DSA perpendicularily. In the right picture of Fig. 2 the translational part of this π-screw is shown. This translation along the DSA moves the rotated triangle (shown in dashed) to the final pose (the point b_1' is translated to the final position B_1).

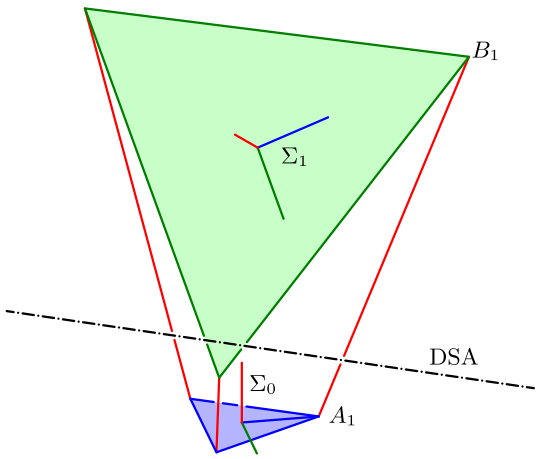

Fig. 3. Solution in the operation mode $\mathbf{V}(\mathcal{K}_2)$.

5.2. The operation mode $\mathbf{V}(\mathcal{K}_2)$

In the operation mode $\mathbf{V}(\mathcal{K}_2)$ every solution has the property $x_1 = 0$. This yields $p_0 = 0$ for the Plücker-coordinates of the DSA for all transformations in this operation mode. The vector $(0,p_1,p_2)$ is representing the direction of the screw axis, which means that all the DSA in this operation mode are parallel to the yz-plane. They intersect the line at infinity of this plane and therefore they are contained in a singular linear line complex. Again, the discrete motion from the identity to the final position of the manipulator is the concatenation of rotation around and a translation along the DSA, but in this case the angle of the rotational part is not necessarily π. An example for this operation mode would be the home pose, which is depicted in Fig. 1.

In the following general example the design parameters are again $h_1 = 1$ and $h_2 = 3$. The joint parameters are chosen: $r_1 = 5.226$, $r_2 = 1$, $r_3 = 5.185$. A solution within this operation mode is $(x_0 : \ldots : y_3) = (3.063 : 0 : .875 : 1.451 : -.034 : -4.819 : 3.517 : -2.049)$. This discrete screw motion is a concatenation of a rotation around the DSA with Plücker-coordinates $(p_0 : \ldots : p_5) = (0 : -2.512 : -4.166 : -13.835 : 10.007 : -6.034)$ with an angle $\varphi = 1.011$ and a translation along the screw axis with translational distance $s = -.040$. This solution is shown in Fig. 3.

5.3. The intersection of the operation modes $\mathbf{V}(\mathcal{K}_1 \cup \mathcal{K}_2)$

The special solutions, which are in the intersection of the two operation modes $\mathbf{V}(\mathcal{K}_1)$ and $\mathbf{V}(\mathcal{K}_2)$, are called *transition poses* between the operation modes. This case will be studied more precisely in Section 6.1. From a geometrical viewpoint the solutions in $\mathbf{V}(\mathcal{K}_1 \cup \mathcal{K}_2) = \mathbf{V}(\mathcal{K}_1) \cap \mathbf{V}(\mathcal{K}_2)$ fulfill the condition $x_0 = x_1 = 0$. This means that all the transformations are π-screws with DSA parallel to the yz-plane. An example with $h_1 = 1$ and $h_2 = 3$ will follow in Section 6.1. A solution for these design parameters is shown in Fig. 4.

6. Singular poses of the manipulator

In this section the singular poses of the 3-RPS parallel manipulator will be discussed. In the kinematic image space the singular poses of both components are computed by taking the Jacobian

$$\mathbf{J}_i = \left(\frac{\partial g_j}{\partial x_k}, \frac{\partial g_j}{\partial y_k} \right)$$

of each system of polynomials $\mathcal{K}_i$ and computing the determinant $S_i : det(\mathbf{J}_i) = 0$. This results in a hyper-variety of degree 8 in each component

$$S_1 : x_1 \cdot p^7(x_2,x_3,y_0,y_1,y_2,y_3) = 0 \quad \text{and} \quad S_2 : x_0 \cdot p^7(x_2,x_3,y_0,y_1,y_2,y_3) = 0. \tag{11}$$

It is obvious from Eq. (11) that the linear space $x_0 = x_1 = 0$ belongs to the singularity variety. A solution is already shown in Fig. 4. The remaining parts in each component are varieties of degree 7.

In mechanics it is desirable to have the singularity surfaces also in the joint space $\mathcal{R}$. Every singular pose of the manipulator has to be a point of the intersection of $\mathbf{V}(\mathcal{K}_i)$ and the variety $\mathbf{V}(\langle S_i \rangle)$. The ideal of singular poses is therefore $\mathcal{S}_i = \mathcal{K}_i \cup \langle s_i \rangle$ and the singular poses are the solutions in $\mathbf{V}(\mathcal{S}_i)$. To obtain the singularity surface in $\mathcal{R}$ the following projection is

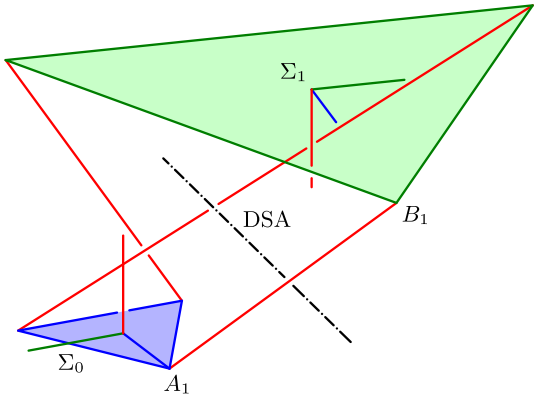

Fig. 4. Assembly mode in $\mathbf{V}(\mathcal{K}_1 \cup \mathcal{K}_2)$.

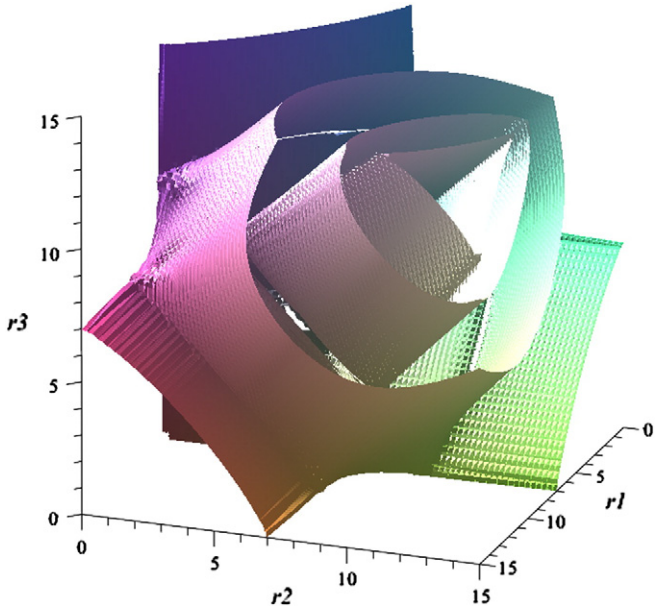

Fig. 5. Singularity surface of $\mathbf{V}(\mathcal{K}_1)$ for $h_1 = 1$, $h_2 = 3$.

defined

$$\iota : \mathcal{S}_i \rightarrow \mathcal{R}, \qquad i \in \{1, 2\},$$

where $\mathcal{R}$ is the polynomial ring over the variables r_1, r_2, r_3. It has to be noted that the joint space $\mathcal{R}$ has two different meanings in this case. On one hand it is a polynomial ring over the variables r_1, r_2, r_3 and on the other hand it is the 3-dimensional joint space, which includes the singularity surfaces. Algebraically this projection is simply the elimination of the remaining Study-parameters and the ideal $\mathcal{S}_i$ will be mapped to the elimination ideal generated by one equation in r_1, r_2, r_3. Now the singularity set consists of surfaces in $\mathcal{R}$. It was not possible to compute this elimination in general, but after assigning arbitrary values to h_2 the computation could be done. For the following example $h_1 = 1$ and $h_2 = 3$ have been assigned. To compute the singularity set of the manipulator in the joint space $\mathcal{R}$, the determinant of the Jacobian of the system $\mathcal{I}$ was added to the original system $\mathcal{I}$. Then $x_0, x_1, x_2, x_3, y_0, y_1, y_2, y_3$ have been eliminated to obtain a polynomial in r_1, r_2, r_3 only. This algorithm was performed for each system $\mathcal{K}_i$ separately. Note that after the elimination only one equation in r_1, r_2, r_3 remains. Geometrically

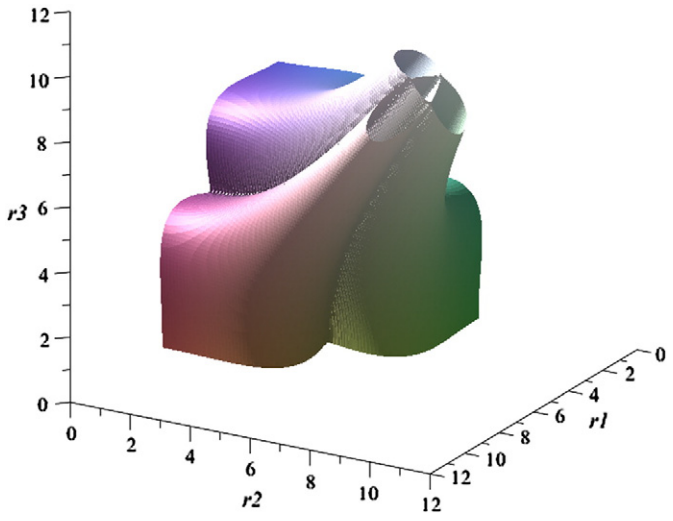

Fig. 6. Singularity surface of $\mathbf{V}(\mathcal{K}_1 \cup \mathcal{K}_2)$ for $h_1 = 1$, $h_2 = 3$.

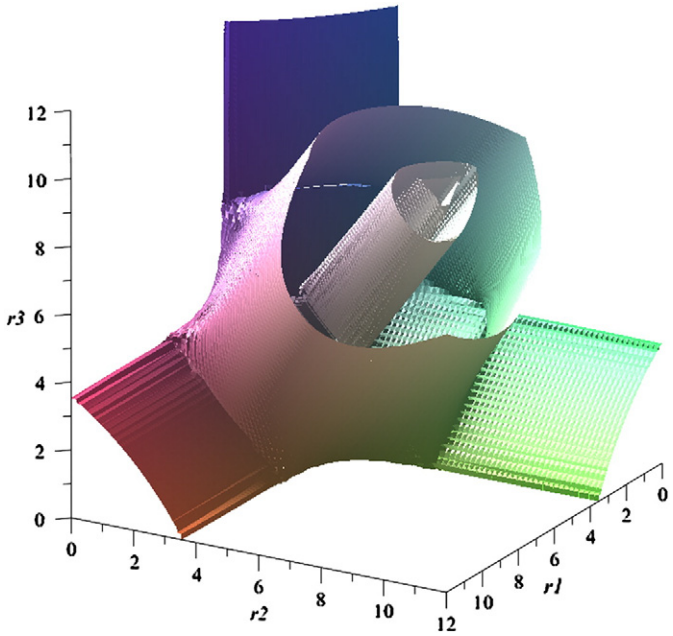

Fig. 7. Singularity surface of $\mathbf{V}(\mathcal{K}_2)$ for $h_1 = 1$, $h_2 = 3$.

this equation represents a surface in the three dimensional joint space. Taking a point on this surface and computing the direct kinematics yield at least one singular pose of the manipulator. Other solutions of the direct kinematics for the chosen set of joint parameters will lead to nonsingular assemblies.

For the system $\mathcal{K}_1$ and the Jacobian J_1 there is the condition $x_0 = 0$. Eliminating the remaining variables $x_1, x_2, x_3, y_0, y_1, y_2, y_3$ leads to a degree 32 polynomial in r_1, r_2, r_3, which factorizes in a product of a degree 24 and a degree 8 polynomial. The corresponding degree 24 surface is shown in Fig. 5 and Fig. 6 shows the degree 8 surface. A similar situation occurs for the system $\mathcal{K}_2$. One obtains again a polynomial of degree 32, that factorizes in a product of a degree 24 and a degree 8 polynomial. The corresponding singularity surface of degree 24 for this component is shown in Fig. 7. The remaining degree 8 surface is the same as in the first case. An interpretation of the common degree 8 factor is given in the next section. The surfaces in

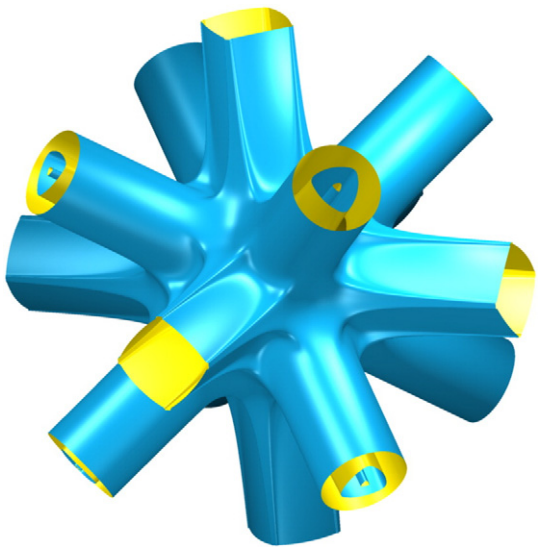

Fig. 8. Singularity surface of $\mathbf{V}(\mathcal{K}_1)$ for $h_1 = 1$, $h_2 = 2$.

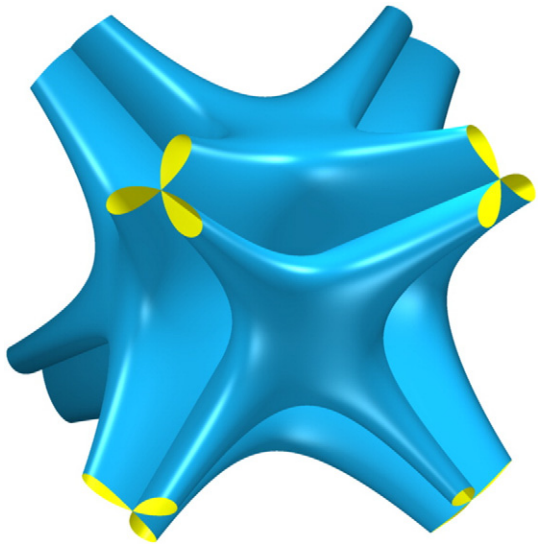

Fig. 9. Singularity surface of $\mathbf{V}(\mathcal{K}_1 \cup \mathcal{K}_2)$ for $h_1 = 1$, $h_2 = 2$.

Figs. 5–7 are plotted in the 3-dimensional joint space $\mathcal{R}$ for the mechanically relevant parts which lie in the first octant of the coordinate system where all r_i are positive.

In a second example $h_1 = 1$ and $h_2 = 2$ are assigned. In Figs. 8–10 the singularity surfaces are depicted. Note that this is a special case, where the singularity surface in Fig. 9 has a self-intersection in the line $r_1 = r_2 = r_3$. The figures show the whole surfaces as obtained by the projection from the kinematic image space to the joint space. The mechanically relevant parts would be in the first octant, where all r_i are positive.

6.1. The transition between the operation modes

In this section the transition between the operation modes will be discussed. To move from one operation mode to the other a solution with $x_0 = x_1 = 0$ has to be passed. From the previous section follows that this solution has to be a singular pose of the manipulator. The computations showed, that the intersection of the degree 32 singularity surfaces in $\mathcal{R}$ is the surface of degree 8

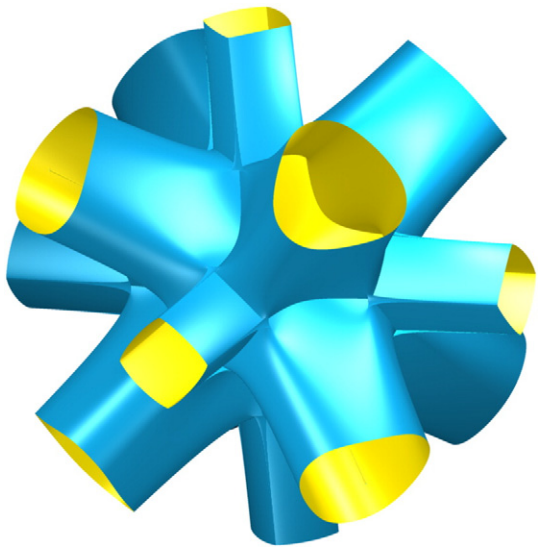

Fig. 10. Singularity surface of $\mathbf{V}(\mathcal{K}_2)$ for $h_1 = 1$, $h_2 = 2$.

Table 1
Stepwise solutions out of a singular assembly mode.

r_3	Operation mode	Study-parameters $(x_0 : \ldots : y_3)$
$\sqrt{21}$	$\mathbf{V}(\mathcal{K}_1 \cup \mathcal{K}_2)$	$(0 : 0 : .092 : .996 : 1.443 : .408 : 1.725 : -.159)$
$\sqrt{21}+\frac{3}{4}$	$\mathbf{V}(\mathcal{K}_1)$	$(0 : -.066 : .0474 : .997 : 1.348 : .212 : 1.998 : -.081)$
	$\mathbf{V}(\mathcal{K}_2)$	$(.309 : 0 : .263 : .914,.863 : .330 : 2.089 : -.891)$
$\sqrt{21}+\frac{3}{2}$	$\mathbf{V}(\mathcal{K}_1)$	$(0 : -.116 : -0.006 : .993 : 1.228 : -0.029 : 2.248 : 0.011)$
	$\mathbf{V}(\mathcal{K}_2)$	$(.404 : 0 : .488 : .774 : -.135 : .213 : 2.231 : -1.337)$

displayed in Eq. (12) for $h_1 = 1$ and general h_2.

$$\begin{aligned} &r_1^8 - 2r_1^6r_2^2 + 3r_1^4r_2^4 - 2r_1^2r_2^6 + r_2^8 - 2r_1^6r_3^2 - 24r_1^6 + 36r_1^4r_2^2 + 36r_1^2r_2^4 - 2r_2^6r_3^2 \\ &\quad - 24r_2^6 + 3r_1^4r_3^4 - 18r_1^4h_2^4 + 36r_1^4r_3^2 + 36r_1^4h_2^2 + 144r_1^4 + 18r_1^2r_2h_2^4 - 144r_1^2r_2^2r_3^2 \\ &\quad - 36r_1^2r_2^2h_2^2 - 144r_1^2r_2^2 + 3r_2^4r_3^4 - 18r_2^4h_2^4 + 36r_2^4r_3^2 + 36r_2^4h_2^2 + 144r_2^4 - 2r_1^2r_3^6 \\ &\quad + 18r_1^2r_3^2h_2^4 + 36r_1^2r_3^4 - 36r_1^2r_3^2h_2^2 - 144r_1^2r_3^2 - 2r_2^2r_3^6 + 18r_2^2r_3^2h_2^4 + 36r_2^2r_3^4 \\ &\quad - 36r_2^2r_3^2h_2^2 - 144r_2^2r_3^2 + r_3^8 - 18r_3^4h_2^4 + 81h_2^8 - 24r_3^6 + 36r_3^4h_2^2 - 972h_2^6 + 144r_3^4 \\ &\quad + 3888h_2^4 - 5184h_2^2 = 0 \end{aligned} \tag{12}$$

There are two possibilities to obtain Eq. (12): First of all one can assign $x_0 = x_1 = 0$ and eliminate the remaining Study-parameters from $\mathcal{I}$, which was used to compute the polynomial for general h_2. The other possibility is to compute the singularity condition for each operation mode separately and take the common factor of degree 8, which is useful to avoid extra elimination time, but in this case h_2 has to be assigned.

In the following example the motion out of a pose in the intersection of the operation modes into the different operation modes for $h_1 = 1$ and $h_2 = 3$ will be shown. Starting point is a singular pose with $x_0 = x_1 = 0$. Assigning $r_1 = r_2 = 6$ and solving Eq. (12) for r_3 yield $r_3 = \sqrt{21}$ to obtain a singular pose. Now the leg lengths which will lead to a singular pose are given but the singular pose within the 16 solutions of the direct kinematics with the given joint parameters has to be found. Fig. 4 shows the computed pose for these parameters. The corresponding Study-parameters are $(x_0 : \ldots : y_3) = (0 : 0 : .092 : .996 : 1.443 : .408 : 1.725 : -.159)$. To move out of this singular pose at least one of the leg lengths has to be changed. In this example r_3 has been extended by a step width $t \in \{\frac{3}{4}, \frac{3}{2}\}$. The new solutions for the leg lengths $r_1 = r_2 = 6$ and $r_3 = \sqrt{21} + t$ are calculated numerically with Newton's method using as starting value the singular solution from above. One solution has to be in the operation mode $\mathbf{V}(\mathcal{K}_1)$, this is the triangle in Σ_1^1, and the other one in $\mathbf{V}(\mathcal{K}_2)$, this is the triangle in Σ_1^2. The solutions of this procedure are collected in Table 1 and the first two steps of the motion are visualized in Fig. 11.

7. Algebraic analysis of the singularity surfaces

In this section the singularity surfaces in $\mathcal{R}$ are analyzed. In case of the singularity surface in the intersection of the operation modes, all the calculations are done for general h_2. This was not possible for the singularity surfaces in the operation modes itself. In this analysis the singularity surfaces for the operation mode $\mathbf{V}(\mathcal{K}_i)$ are denoted Φ_i, the singularity surface in the intersection is denoted Φ_{12}.

7.1. Algebraic analysis of Φ_{12}

Φ_{12} is an algebraic surface of degree 8 for every h_2, given by Eq. (12). To handle the points at infinity of this surface it is useful to homogenize the equation, introducing $r_i = \frac{R_i}{R_0}$ $(i \in \{1,2,3\})$. After normalizing and removing the common denominator the homogeneous equation reads

$$\begin{aligned} &36R_1^4h_2^2R_0^4 + 36R_2^4R_3^2R_0^2 - 36R_1^2R_3^2h_2^2R_0^4 + 18R_1^2R_3^2h_2^4R_0^4 - 36R_1^2R_2^2h_2^2R_0^4 - \\ &36R_2^2R_3^2h_2^2R_0^4 + 18R_2^2R_3^2h_2^4R_0^4 + 18R_1^2R_2^2h_2^4R_0^4 - 144R_1^2R_2^2R_3^2R_0^2 + 36R_2^4h_2^2R_0^4 - \\ &144R_2^2R_3^2R_0^4 - 144R_1^2R_2^2R_0^4 - 144R_1^2R_3^2R_0^4 - 18R_1^4h_2^4R_0^4 + 36R_2^2R_3^4R_0^2 + \\ &36R_1^2R_2^4R_0^2 + 36R_1^2R_3^4R_0^2 - 18R_2^4h_2^4R_0^4 + 36R_3^4h_2^2R_0^4 + 36R_1^4R_2^2R_0^2 + \\ &36R_1^4R_3^2R_0^2 - 18R_3^4h_2^4R_0^4 + 81h_2^8R_0^8 - 972h_2^6R_0^8 + 144R_2^4R_0^4 + 144R_1^4R_0^4 + \\ &3R_1^4R_3^4 - 2R_1^6R_3^2 - 2R_2^2R_3^6 + 3R_1^4R_2^4 - 2R_1^6R_3^2 + 3R_2^4R_3^4 - 2R_2^6R_3^2 - 2R_1^2R_2^6 - \\ &2R_1^6R_2^2 - 24R_2^6R_0^2 - 24R_1^6R_0^2 - 24R_3^6R_0^2 + 144R_3^4R_0^4 + 3888h_2^4R_0^8 - 5184h_2^2R_0^8 + \\ &R_1^8 + R_2^8 + R_3^8 = 0. \end{aligned} \tag{13}$$

The intersection curve of Φ_{12} with the plane at infinity $R_0 = 0$ is a double covered curve of degree 4 represented by Eq. (14). Note

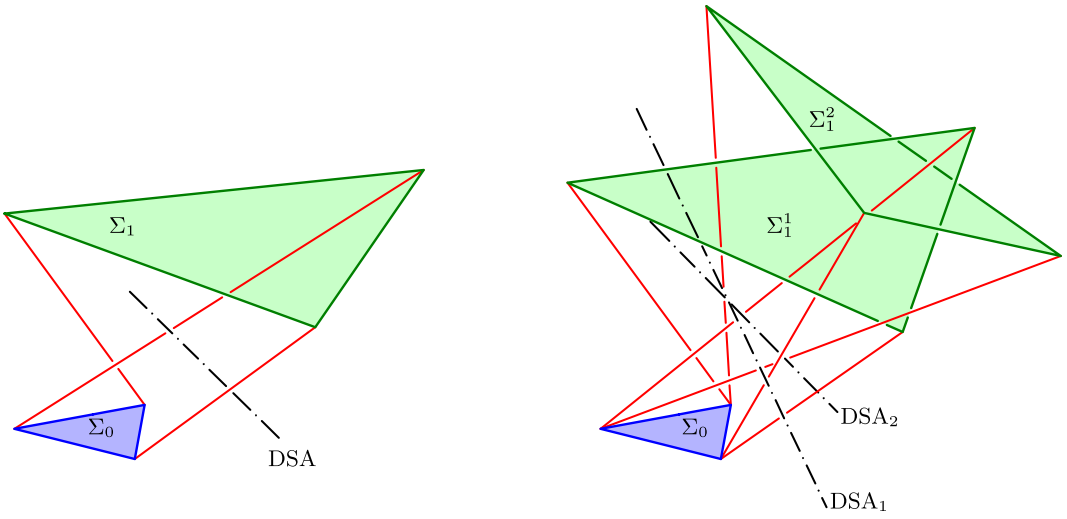

Fig. 11. Moving out of a singular pose.

that this curve is independent of h_2. This means that the intersection curve is the same for all manipulators.

$$\left(R_1^4 - R_1^2R_2^2 + R_2^4 - R_1^2R_3^2 - R_2^2R_3^2 + R_3^4\right)^2 = 0 \tag{14}$$

The curve given in Eq. (14) splits into two double covered complex conics c_1 and c_2

$$\begin{aligned} c_1 &: -2R_1^2 + R_2^2 + R_3^2 + i\sqrt{3}\left(R_2^2 - R_3^2\right) = 0 \\ c_2 &: -2R_1^2 + R_2^2 + R_3^2 - i\sqrt{3}\left(R_2^2 - R_3^2\right) = 0. \end{aligned} \tag{15}$$

Although the conics c_1 and c_2 are complex, they intersect in 4 real points with homogeneous coordinates $(0:1:1:1)$, $(0:-1:1:1)$, $(0:1:-1:1)$ and $(0:1:1:-1)$. Each of the four intersection points has algebraic multiplicity 4, because both curves c_1 and c_2 are double covered. To visualize the situation within the plane at infinity $R_0 = 0$ a change of coordinates is applied. By interchanging the coordinates R_3 and R_0 the new plane at infinity becomes $R_3 = 0$. In Fig. 13 and Fig. 12 the singularity surface is depicted after assigning $R_3 = 1$. The former plane at infinity has become a proper plane and the behavior of the surface can be visualized. The above discussed intersection points appear as conic nodes within the proper plane $R_0 = 0$.

To find all the singular points and curves on this surface, the partial derivatives of Eq. (13) are computed. A point on a surface is *singular*, if all the partial derivatives and the surface equation vanish simultaneously. In terms of algebraic geometry this means

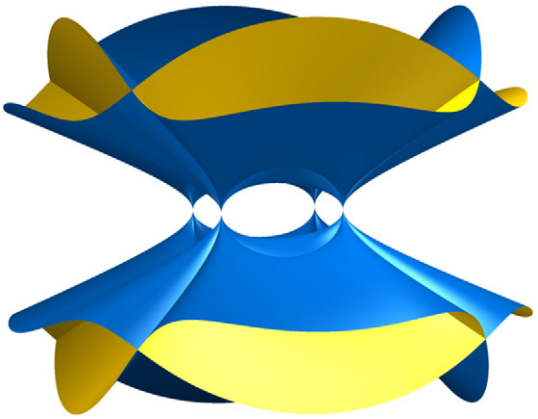

Fig. 12. The singularity surface Φ_{12} from a different point of view ($h_2 = 3$).

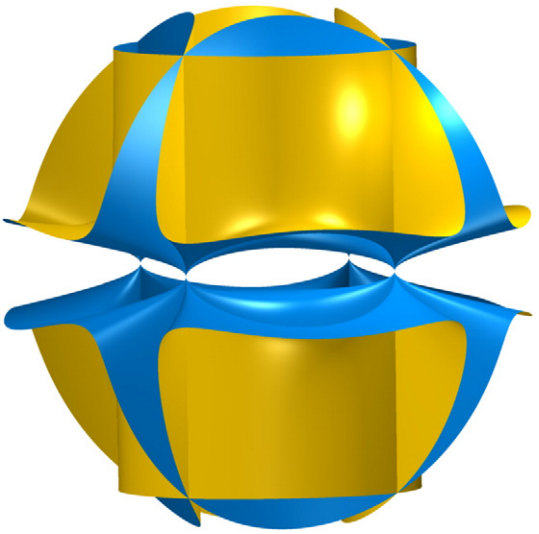

Fig. 13. The singularity surface Φ_{12} from a different point of view ($h_2 = 2$).

that the point lies in the vanishing set of the ideal generated by the partial derivatives and the surface equation. For this ideal a Gröbner basis can be calculated. It turns out that the 16 points at infinity are singular points on the surface.

In the proper part of the space, there are 12 hyperbolas on the surface, which are carrying singular points. These hyperbolas appear as the intersection of the planes with $R_1 = \pm R_3$ resp. $R_1 = \pm R_3$ resp. $R_2 = \pm R_3$ and the hyperbolic cylinders with $3h_2^2 - 12 + R_2^2 - R_3^2 = 0$ resp. $3h_2^2 - 12 + R_2^2 - R_3^2 = 0$ resp. $3h_2^2 - 12 - R_3^2 + R_1^2 = 0$. This general case is depicted in Fig. 6 and Fig. 12. A special case appears when $h_2 = 2$, then the hyperbolic cylinders degenerate into pairs of planes and the 12 hyperbolas become 4 lines, those are the lines $R_1 = \pm R_2 = \pm R_3$. This special case can be seen in Fig. 9 and Fig. 13, where all the branches intersect in this special lines.

7.2. Algebraic analysis of Φ_1 and Φ_2

As in the previous section the singularity surfaces Φ_1 and Φ_2 are intersected with the plane at infinity. After homogenizing the degree 24 equations and setting $R_0 = 0$ the intersection curve of Φ_1 and the plane at infinity is given by

$$\left(R_1^4R_2^4 + R_2^4R_3^4 - R_1^2R_2^4R_3^2 - R_1^4R_2^2R_3^2 - R_1^2R_2^2R_3^4 + R_1^4R_3^4\right)^2\left(R_1^4 - R_1^2R_2^2 + R_2^4 - R_1^2R_3^2 - R_2^2R_3^2 + R_3^4\right)^2 = 0. \tag{16}$$

The same polynomial is obtained by intersecting Φ_2 with the plane at infinity. The second factor in Eq. (16) is the same as in Eq. (14), so again both surfaces have the four-fold points at infinity $(0:1:1:1)$, $(0:-1:1:1)$, $(0:1:-1:1)$ and $(0:1:1:-1)$. The first factor of Eq. (16) is also complex, but it has 3 real points, namely $(0:1:0:0)$, $(0:0:1:0)$ and

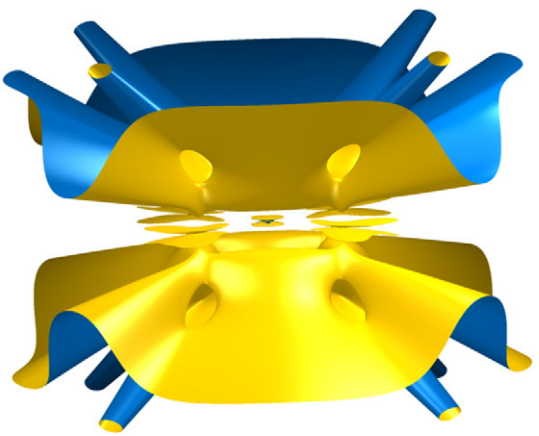

Fig. 14. The singularity surface Φ_1 from a different point of view.

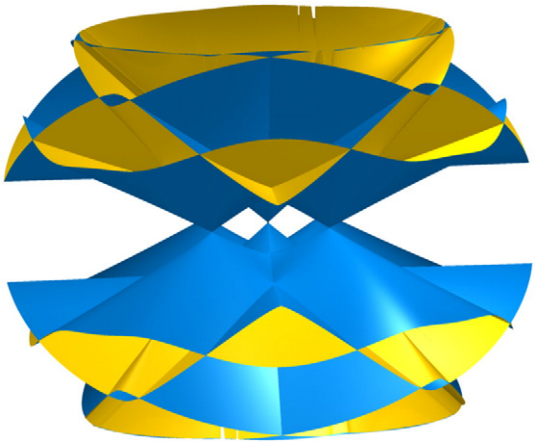

Fig. 15. The singularity surface Φ_2 from a different point of view.

$(0:0:0:1)$. The points are the points at infinity of the r_1, r_2 and r_3 coordinate axes. Fig. 14 and Fig. 15 show the surfaces after the coordinate transformation which maps the plane at infinity to a proper plane. The points at infinity are then the conic nodes of the surface.

8. Conclusion

In this paper it was shown, that an algebraic approach to the analysis of the 3-RPS parallel manipulator yields new global kinematic properties. Primary decomposition of the ideal of constraint equations revealed two kinematically different operation modes of the manipulator. Both operation modes were characterized geometrically as well as kinematically. It was shown that the direct kinematics can be solved in closed form without specifying the design parameters and the theoretical number of 16 solutions was confirmed. In discussing the Jacobian of the two sets of constraint equations a complete description of all singular poses of the manipulator was obtained in the kinematic image space. The singularity sets corresponding to the two operation modes intersect and this intersection is used to show that a transition from one operation mode into the other is possible. A projection of the singular set into the joint space yields the singularity set in the joint space. The resulting algebraic surfaces are discussed in detail. Based on the algebraic representation presented in this paper a complete description of all self-motions of this manipulator [21] is possible.

References

[1] K.H. Hunt, Structural kinematics of in-parallel-actuated robot-arms, Trans. ASME J. Mech. Transm. Autom. Des. vol. 105 (1983) 705–712.
[2] L.-W. Tsai, Robot Analysis, John Wiley and Sons, Inc., 1999
[3] P. Nanua, K.J. Waldron, V. Murthy, Direct kinematic solution of a Stewart platform, IEEE Trans. Robot. Autom. 6 (4) (1990) 438–444.
[4] J. Gallardo, H. Orozco, J. Rico, C. Aguilar, L. Perez, Acceleration analysis of 3-RPS parallel manipulators by means of screw theory, in: J.–H. Ryu (Ed.), Parallel Manipulators, New Developments, I-Tech Education and Publishing, 2008, pp. 315–330.
[5] I.A. Bonev, Direct kinematics of zero-torsion parallel manipulators, Proceedings of 2008 IEEE International Conference on Robotics and Automation, Pasadena, CA, USA, 2008, pp. 3851–3856.
[6] Y. Fang, Z. Huang, Kinematics of a three-degree-of-freedom in-parallel actuated manipulator mechanism, Mech. Mach. Theory 32 (1997) 789–796.
[7] O. Ibrahim, W. Khalil, Kinematic and dynamic modeling of the 3-RPS parallel manipulator, Proceedings of the 12th IFToMM World Congress, Besancon (France), 2007.
[8] A. Sokolov, P. Xirouchakis, Kinematics of a 3-DOF parallel manipulator with an R-P-S joint structure, Robotica 23 (2005) 207–217.
[9] B. Dasgupta, P. Choudhury, A general strategy based on the Newton–Euler approach for the dynamic formulation of parallel manipulators, Mech. Mach. Theory 34 (1999) 801–824.
[10] Y. Song, Y. Li, T. Huang, Inverse dynamics of 3-RPS parallel mechanism based on virtual work principle, Proceedings of the 12th IFToMM World Congress, Besancon (France), 2007.
[11] N. Farhat, V. Mata, A. Page, F. Valero, Identification of dynamic parameters of a 3-DOF RPS parallel manipulator, Mech. Mach. Theory 43 (2008) 1–17.
[12] Z. Huang, J. Wang, Y.F. Fang, Analysis of instantaneous motions of deficient-rank 3-RPS parallel manipulators, Mech. Mach. Theory 37 (2002) 229–240.
[13] Z. Huang, J. Wang, Identification of principal screws of 3-DOF parallel manipulators by quadric degeneration, Mech. Mach. Theory 36 (2001) 893–911.
[14] Z. Huang, W.S. Tao, Y.F. Fang, Study on the kinematic characteristics of 3 DOF in-parallel actuated platform mechanisms, Mech. Mach. Theory 31 (1996) 999–1007.
[15] N. Mohan Rao, K. Mallikarjuna Rao, Dimensional synthesis of a spatial 3-RPS parallel manipulator for a prescribed range of motion of spherical joints, Mech. Mach. Theory 44 (2009) 477–486.
[16] Y. Lu, T. Leinonen, Solution and simulation of position–orientation for multi-spatial 3-RPS parallel mechanisms in series connection, Multibody System Dynamics, vol. 142005. 47–60.
[17] D. Basu, A. Ghosal, Singularity analysis of platform-type multi-loop spatial mechanisms, Mech. Mach. Theory 32 (1997) 375–389.
[18] D. Zlatanov, I.A. Bonev, C.M. Gosselin, Constraint singularities of parallel mechanisms, Proceedings of the 2002 IEEE International Conference on Robotics and Automation, Washington, 2002, pp. 496–502.
[19] A. Sokolov, P. Xirouchakis, Singularity analysis of a 3-DOF parallel manipulator with an R-P-R joint structure, Robotica 24 (2006) 131–142.
[20] C.H. Liu, S. Cheng, Direct singular positions of a 3RPS parallel manipulator, Trans. ASME 126 (2004) 1006–1016.

[21] M.L. Husty, J. Schadlbauer, S. Caro, P. Wenger, Self-motions of 3-RPS manipulators, in: F. Viadero, M. Ceccarelli (Eds.), New Trends in Mechanism and Machine Science, Theory and Application in Engineering, Mechanism and Machine Science, 7, Springer-Verlag, 2012, pp. 121–130.
[22] M.L. Husty, M. Pfurner, H.-P. Schröcker, K. Brunnthaler, Algebraic methods in mechanism analysis and synthesis, Robotica 25 (6) (2007) 661–675.
[23] M.L. Husty, An algorithm for solving the direct kinematics of general Stewart–Gough platforms, Mech. Mach. Theory 31 (4) (1996) 365–380.
[24] M.L. Husty, A. Karger, H. Sachs, W. Steinhilper, Kinematik und Robotik, Springer, 1997.
[25] D.R. Walter, M.L. Husty, On implicitization of kinematic constraint equations, Mach. Des. Res. 26 (2010) 218–226.
[26] D. Cox, J. Little, D. O'Shea, Ideals, Varieties, and Algorithms, Springer, 2006.
[27] W. Decker, G.-M. Greuel, G. Pfister, H. Schönemann, SINGULAR 3-1-6—a computer algebra system for polynomial computations, 2012.
[28] E.A. Weiss, Einführung in die Liniengeometrie und Kinematik. B.G. Teubner Leibzig, 1935.
[29] H. Pottmann, J. Wallner, Computational Line Geometry, Springer-Verlag, 2001.
[30] E. Study, Geometrie der Dynamen. Teubner, Leibzig, 1903.